NOTICE CONCERNING COPYRIGHT RESTRICTIONS

ANISOTROPIC RESISTIVITY INVERSION OF VES CURVES AT HATCHOBARU GEOTHERMAL FIELD, JAPAN

Keisuke Ushijima * Kozo Yuhara * Koichi Tagomori ** Kimito Inoue ***

* Mining Department, Kyushu University 36, Fukuoka, Japan
** Geothermal Department, West JEC, Sunselco 10F,Fukuoka,Japan
*** Thermal Power Department, Kyushu Electric Power Co.,Fukuoka,Japan

ABSTRACT

A new method of interpretation of vertical resistivity sounding curves is presented based on an anisotropic layered earth model.

The method has been applied to the VES data in the vicinity of production region and a virgin area in the Hatchobaru geothermal field. The results of interpretation are compared with the drilling data from the production wells.

Concludingly, an acceptable geoelectric model was obtained for the hydrothermal system at the Hatchobaru area.

In addition, it was proved that anisotropic coefficients determined from the resistivity inversion provide the valuable information not only on the true resistivity layer section, but on the estimation of fractures which are the vertical or the horizontal ones. From this study, it was found that most of production wells located near the VES stations in the domain IV in the anisotropic coefficient map.

INTRODUCTION

The anisotropic charactor of the formation has been generally overlooked in the interpretation of resistivity sounding curves, though geological formations may have the different resistivity values along the parallel direction and in the normal direction to the bedding planes. This phenomenon is quite common in various formations such as not only sedimentary beds but fractured igneous beds having contrasting lithologies. It is also well known as a traditional problem that the application of the interpretation method based on an isotropic layering to the resistivity sounding (VES) curves leads to substantial errors if the subsurface formations were shown to be anisotropic.

Jupp and Vozoff(1977) has shown that the anisotropy could be resolved with joint inversion of DC resistivity and magnetotelluric data, because the MT measurements responds only to conductivity and depth estimates are not distorted.

In the present paper, we have demonstrated that the anisotropy in each layer unit of the subsurface formations could be separately determined from the usual VES curves obtained in the field survey by means of a least-squares inversion techniques.

The new method of interpretation based on the anisotropic layered earth is applied to the VES data which were previously obtained at the Hatchobaru geothermal field in Japan.

FORWARD PROBLEM

We consider an anisotropic half space made up of a layered earth illustrated by Fig.1.

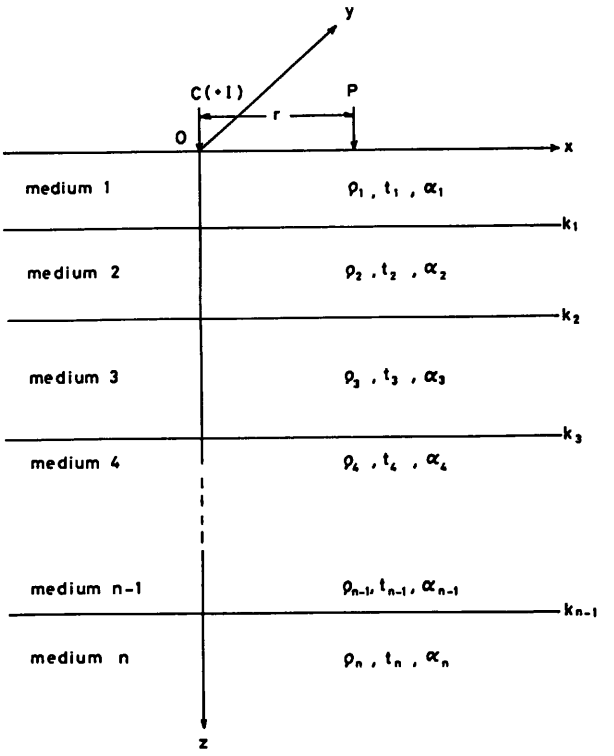

Fig. 1. Anisotropic layered earth model that has the different resistivity values along the parallel direction and in the normal direction to the bedding planes.

Considering the layering to be horizontal, we shall denote the resistivity to current in the direction perpendicular to the layering ρ_t and the resistivity to current along the strata ρ_ℓ.

Furthermore, we shall introduce the concepts of average resistivity ρ_m , defined as

$$\rho_m = \sqrt{\rho_\ell \cdot \rho_t} \qquad (1)$$

and coefficient of anisotropy, α defined as

$$\alpha = \sqrt{\rho_t / \rho_\ell} = \sqrt{\sigma_\ell / \sigma_t} \qquad (2)$$

where σ is the conductivity and the quantity α is a measure of the anisotropy.

In conditions where the potential field has a cylindrical symmetry and the anisotropy is of the type refered to above, the relation that must be satisfied is thus

$$\frac{1}{\rho_\ell}\left(\frac{\partial^2 V}{\partial r^2} + \frac{1}{r}\frac{\partial V}{\partial r}\right) + \frac{1}{\rho_t}\frac{\partial^2 V}{\partial z^2} = 0 \qquad (3)$$

or

$$\frac{\partial^2 V}{\partial r^2} + \frac{1}{r}\frac{\partial V}{\partial r} + \frac{1}{\alpha^2}\frac{\partial^2 V}{\partial z^2} = 0 \qquad (4)$$

In particular, the expression for the potential , caused by a point source of current at the surface of a homogeneous but anisotropic earth must be

$$V = \frac{\rho_{1m} I}{2\pi\sqrt{r^2 + (\alpha z)^2}} \qquad (5)$$

where I is the intensity of the electric current.

The particular solutions of the equation (4) must then be

$$V = C\, e^{-\lambda\alpha z} J_0(\lambda r) \quad \text{and} \quad V = C\, e^{+\lambda\alpha z} J_0(\lambda r) \qquad (6)$$

Using eqs.(5) and (6) the general solution in the i-th layer, can be written

$$V_i = \frac{\rho_{1m} I}{2\pi}\left\{\frac{1}{\sqrt{r^2+\alpha_i^2 z^2}} + \int_0^\infty \{L_i(\lambda)e^{\lambda\alpha_i z} + M_i(\lambda)e^{-\lambda\alpha_i z}\}J_0(\lambda r)d\lambda\right\} \qquad (7)$$

where, J_0 is the Bessel function of zero order.

We introduce a modified depth coordinate, h which defined by Koefoed(1979) as

$$h = \int_0^z d(\alpha z) \qquad (8)$$

and the integral of Lipschitz:

$$\int_0^\infty e^{-\lambda z} J_0(\lambda r)\, d\lambda = \frac{1}{\sqrt{r^2 + z^2}}$$

then, eq.(7) reduces to

$$V_i = \frac{\rho_{1m} I}{2\pi}\int_0^\infty \{e^{-\lambda h} + L_i(\lambda)e^{\lambda h} + M_i(\lambda)e^{-\lambda h}\}J_0(\lambda r)d\lambda \qquad (9)$$

The functions $L_i(\lambda)$ and $M_i(\lambda)$ are different for the different layers, and are determined by the following boundary conditions.

(I) At the surface, the normal current density must be zero:

$$\frac{\partial V_1}{\partial z} = 0 \quad \text{at} \quad z = 0 \qquad (10)$$

(II) At the boundary between each pair of successive layers two boundary conditions must be satisfied:

$$\left.\begin{aligned} V_i &= V_{i+1} \\ \frac{1}{\rho_{it}}\frac{\partial V_i}{\partial z} &= \frac{1}{\rho_{i+1t}}\frac{\partial V_{i+1}}{\partial z} \end{aligned}\right\} \text{at} \quad z = h_i \qquad (11)$$

(III) At the infinite depth, the potential, that is caused by a current source at the surface, must become zero:

$$V_n = 0 \quad \text{at} \quad z = \infty \qquad (12)$$

These results of the investigation may be summarized by the following system of equations:

$$\begin{aligned} &L_1(\lambda) = M_1(\lambda) \\ &e^{-\lambda h_i}M_i(\lambda) + e^{\lambda h_i}L_i(\lambda) - e^{-\lambda h_i}M_{i+1}(\lambda) - e^{\lambda h_i}L_{i+1}(\lambda) = 0 \\ &-e^{-\lambda h_i}M_i(\lambda) + e^{\lambda h_i}L_i(\lambda) + \kappa_i e^{-\lambda h_i}M_{i+1}(\lambda) - \kappa_i e^{\lambda h_i}L_{i+1}(\lambda) \\ &\qquad = (1-\kappa_i)e^{-\lambda h_i} \\ &L_n(\lambda) = 0 \end{aligned} \qquad (13)$$

where $$\kappa_i = \frac{\alpha_{i+1}}{\rho_{(i+1)t}} \Big/ \frac{\alpha_i}{\rho_{it}} = \rho_{im} / \rho_{(i+1)m} \qquad (14)$$

Eq.(13) is a linear system of 2n equations in the 2n unknowns $L_1, L_2, \ldots, L_n, M_1, M_2, \ldots, M_n$. Since the number of equations is equal to the number of unknown this system can be solved.

The only one of these unknowns, that is of interest, is L_1 because the potential measurements are made at the surface. In the following L_1 will be denoted $R_n(\lambda)$ which is commonly refered to as the kernel function.

The kernel function for an anisotropic layered earth can be written as

$$R_n(\lambda) = \frac{P_n(\lambda)}{Q_n(\lambda)} = \frac{P_n(\lambda)}{H_n(\lambda) - P_n(\lambda)} \qquad (15)$$

where the functions $P_n(\lambda)$, $Q_n(\lambda)$ and $H_n(\lambda)$ may be given by the Flathe's recursion formula:

$$\begin{aligned} P_n(u) &= P_{n-1}(u) + H_{n-1}(1/u)k_{n-1}u^{h_{n-1}} \\ H_n(u) &= H_{n-1}(u) + P_{n-1}(1/u)k_{n-1}u^{h_{n-1}} \\ Q_n(u) &= Q_{n-1}(u) - Q_{n-1}(1/u)k_{n-1}u^{h_{n-1}} \end{aligned} \qquad (16)$$

with $u = \exp(-2\lambda)$.

where the resistivity reflection coefficient and the modified depth are defined by the following equations:

$$k_i = \frac{1-\kappa_i}{1+\kappa_i} = \frac{\rho_{(i+1)m} - \rho_{im}}{\rho_{(i+1)m} + \rho_{im}} \qquad (17)$$

and

$$h_i = \sum_{j=1}^{j=i} \alpha_j t_j \,, \quad i = 1,2,\ldots,n-1. \qquad (18)$$

Therefore , the electric potential at the surface by a point source of electric current is given by the equation

$$V(r,0) = \frac{\rho_{1m} I}{2\pi}\left\{\frac{1}{r} + 2\int_0^\infty R_n(\lambda)J_0(\lambda r)d\lambda\right\} \qquad (19)$$

We thus obtain the mathematical expression for the apparent resistivity for the Schlumberger configuration

$$\rho_a = \rho_{1m}\left\{1 + \frac{L^2}{2}\int_0^\infty R_n(\lambda)J_1(\lambda\tfrac{L}{2})\lambda d\lambda\right\} \qquad (20)$$

where L is the current electrode separation, J_1 is the Bessel function of the first order and $R_n(\lambda)$, the kernel function, is determined by eq.(15).

Eq.(20) makes it possible to compute the apparent resistivity when the kernel is known.

INVERSE PROBLEM

Various authors have published the methods of automatic iterative interpretation, in which the layer parameter adjustment are made by the computer, starting with initial guess parameters. These methods are at present the most excellent tool in the exact interpretation of resistivity sounding measurements. We have used a modified program from the program coded by Ushijima(1980) which numerically accomplish the inversion in a stable manner.

The present computer program has the following features:

(1) The program has used the SALS program as a main program in which Fletcher's algorithm has been used to select an appropriate value for Marquardt's factor at each step of inversion process.
(2) Theoretical apparent resistivity values are calculated for the actual electrode separations taken in the field, using the Johansen's digital filter coefficients.
(3) The weights of the VES data are adjusted according to the residual values between the observed and calculated, based on the robust estimation method.
(4) Statistical estimates of the solutions are made by the informations such as a standard deviation S, Akaike's Information Criterion (AIC), the parameter correlation coefficients, the parameter standard deviations, etc.
(5) The program can be directly applicable to an isotropic case, by fixing the anisotropic coefficient of each layer to equal one.

FIELD EXAMPLES

A series of resistivity sounding measurements has been carried out for the purpose of geothermal resources investigation at the Hatchobaru field. In this survey, data are taken along parallel lines spaced 200 m apart and depth soundings are also made 200 m apart along these lines, with maximum current electrode expansion to 2000 m.

The location of the sounding stations are shown on the maps of Fig.2 together with the location of the production wells.

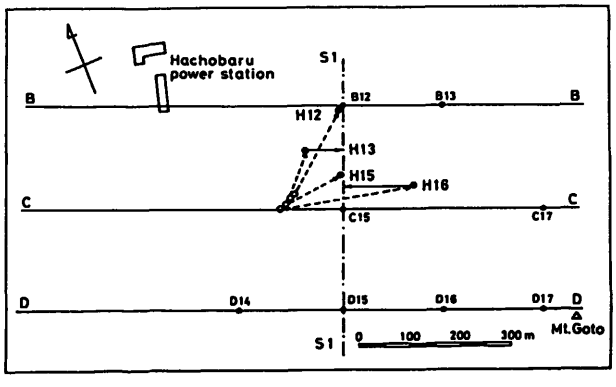

Fig. 2. VES stations and location of production wells at the Hatchobaru geothermal field.

We shall now consider the interpretation of the apparent resistivity curves at three stations B-12, C-15 and D-15, along the line S1, going from northeast to southwest. Line S1 crosses the central portion of the present production zone.

The observed apparent resistivity curves with their interpretation and automatic plotting are shown in Figs. 3 - 5.

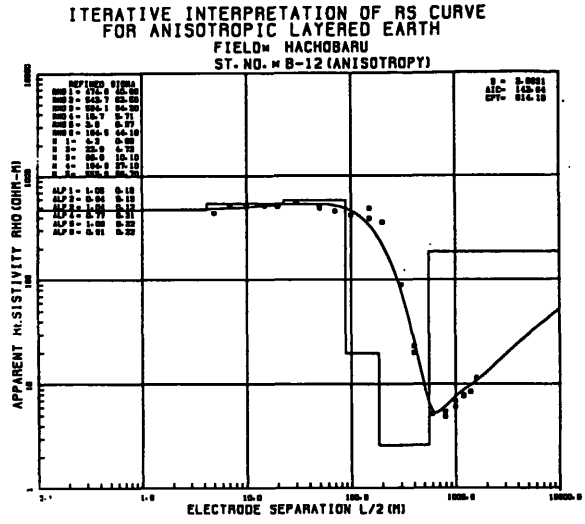

Fig. 3a. VES curve with the interpretation at B-12 (6 layer model).

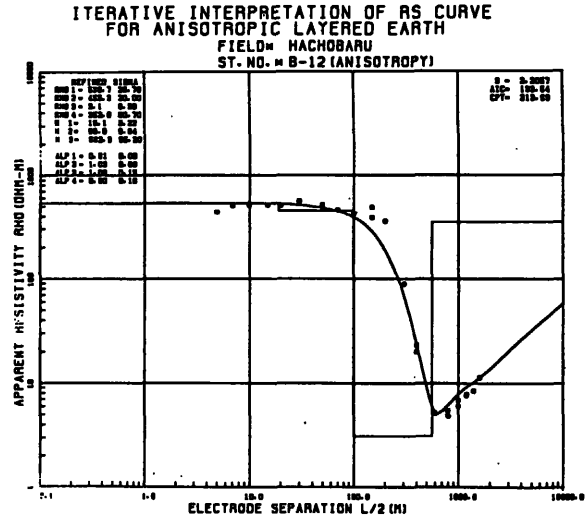

Fig. 3b. VES curve with the interpretation at B-12 (4 layer model).

In these figures, circles show the observed apparent resistivity values and a solid curve represents the theoretical curve obtained by the use of the final solution.

VES curve at B-12 are interpreted in two models, that is as 6-layer curve or 4-layer curve. It is, however interesting to note that the two different models also yield the almost same solution concerning the resistivity values of the low resistivity

zone and the electrical basement and the boundary depth between them due to the high resistivity contrast of them.

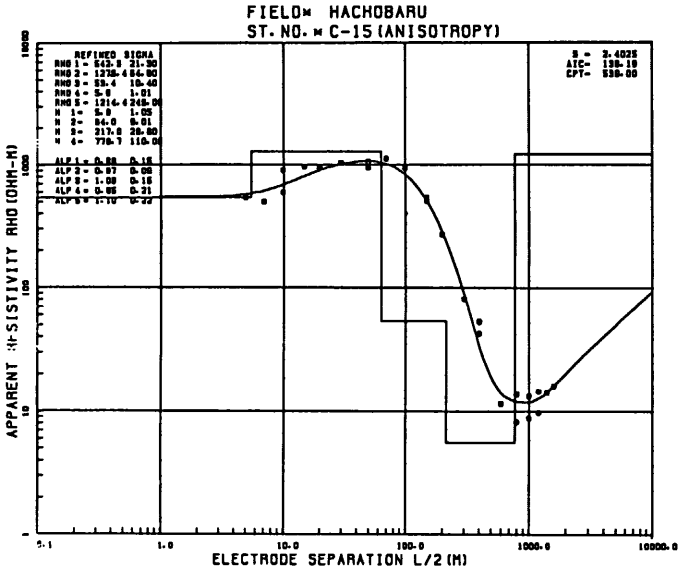

Fig. 4. VES curve with the interpretation at C-15.

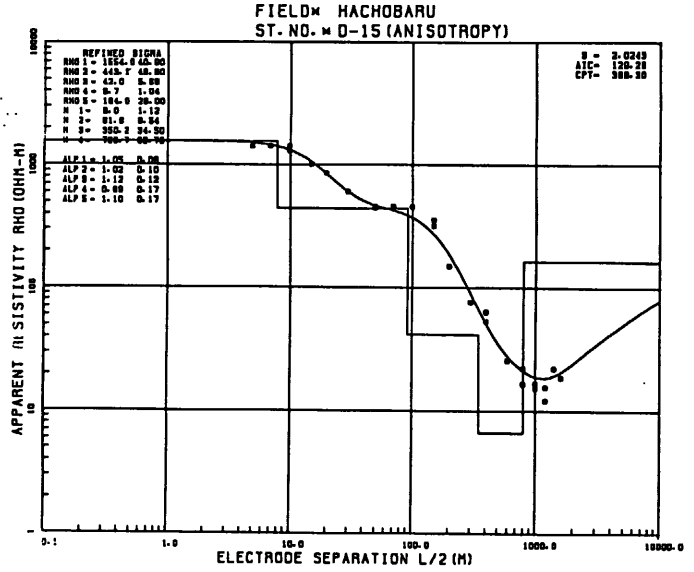

Fig. 5. VES curve with the interpretation at D-15.

Soundings B-12 and C-15 are made in the vicinity of the present production region, then the inversion results of VES curves at these stations will be compared with the drilling data.

COMPARISON OF SOLUTIONS WITH DRILLING DATA

The two types of solutions based on an anisotropic and an isotropic layering are compared with the drilling data along the section projected to the line S1 shown in Fig.2.

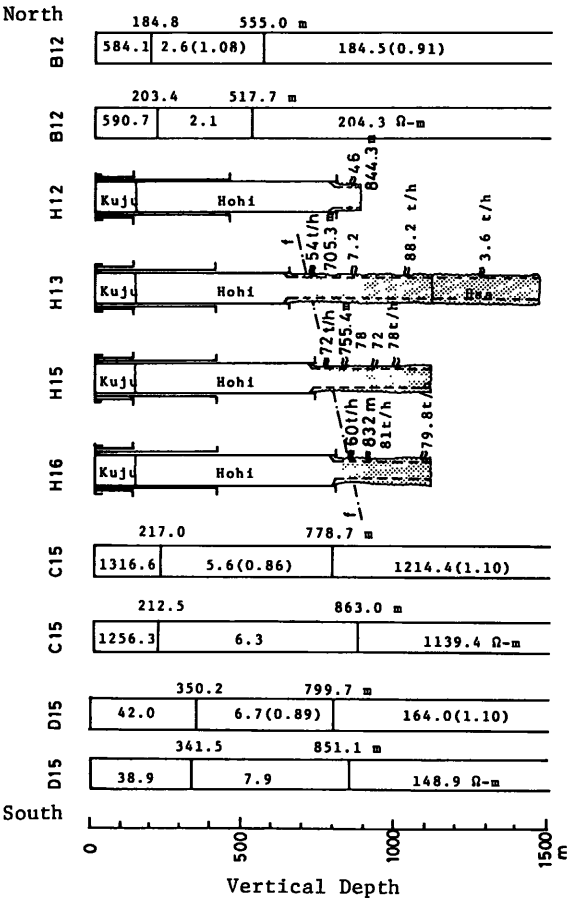

Fig. 6. Comparison of the resistivity layer section along the S1 line with the drilling data of production wells. Values in the parenthesis denote an anisotropic coefficients.

Figure 6 shows the three primary rock units: first, the surface zone with a high resistivity rocks of 500 - 1300 ohm-m that were correlated with volcanic rocks of the Kujyu and upper Hohi sequence ; second, the intermediate layer with the low resistivity rocks of 2.1 - 6.3 ohm-m that were correlated with a section consisting primarily of Pleistocene tuff breccia of the middle Hohi group and fractured volcanics of the lower Hohi sequence; and third, an electrical basement which has a high resistivity between 180 - 1200 ohm-m beneath the low resistivity section which appears to be correlated with the Pyroxene andesite lower Hohi volcanic sequence, the Usa group.

Laterally, with regard to the low resistivity zone, the resistivity takes gradually a high value from B-12 to D-15, that is north to south. This trend coincides with the inclination of faults or the distribution of the lost circulation zone that corresponds to the geothermal reservoir.

In addition, it is also recognized that the marked discontinuity of the depth to the electrical basement exists between B-12 and C-15, thus such a

large discontinuity must be considered to indicate the presence of fault marked by f in Fig.6.

Judging from these three factors, that are the resistivity changes of vertical and lateral directions and the discontinuity of the electrical basement, the location and inclination of fault which regulate the upstream of the geothermal fluid could be determined.

In planning drilling operations, it is important to know the depth to the geothermal reservoir , as well as the lateral boundary. Then, we compare the depth to the electrical basement with the depth of the geothermal reservoir, being shown as the underlined figures in Table 1.

Table 1. Casing program, Lost circulation data, and Well characteristics of production wells at Hatchobaru geothermal field.

Well	Casing Program	Lost Circulation Zone	Well Characteristics
H-12	22" 25.0 m 17 5/8" 130.0 m 11 3/4" 450.9 m 8 5/8" 800.2 m 7 5/8" 871.8 m (liner)	90 t/h 8.9 m 90 t/h 170.0 m 90 t/h 197.0 m 46 t/h 844.3 m* 66 t/h 853.0 m	steam 32.3 t/h water 11.6 t/h ratio 0.36 output 4800 KW
H-13	22" 24.0 m 17 5/8" 131.0 m 11 3/4" 391.2 m 8 5/8" 647.6 m 6" 1455.5 m	76.8 t/h 581.0 m 56 t/h 703.3 m* 7.2 t/h 844.0 m 88.2 t/h 1016.0 m 3.6 t/h 1264.0 m	steam 30.4 t/h water 84.7 t/h ratio 2.79 output 5090 KW
H-15	22" 20.5 m 17 5/8" 130.0 m 11 3/4" 404.5 m 8 5/8" 736.2 m 6" 1097.8 m	90 t/h 12.0 m 90 t/h 42.5 m 96 t/h 391.3 m 77 t/h 723.0 m 72 t/h 755.4 m* 78 t/h 814.0 m 72 t/h 919.6 m 78 t/h 977.0 m	steam 30.5 t/h water 116.4 t/h ratio 3.82 output 5390 KW
H-16	22" 25.0 m 17 5/8" 132.0 m 11 3/4" 411.7 m 8 5/8" 798.6 m 6" 1098.0 m	90 t/h 8.9 m 90 t/h 70.0 m 30 t/h 89.4 m 72 t/h 138.9 m 4.5 t/h 733.0 m 60 t/h 832.0 m* 81 t/h 834.0 m 5.4 t/h 890.0 m 64.8 t/h 1076.4 m 79.8 t/h 1077.4 m	steam 36.5 t/h water 88.5 t/h ratio 2.42 output 5990 KW

It is found that the depth of the electrical basement correlate well with the upper depth of the geothermal reservoir. Therefore, it could be defined that the depth to the electrical basement gives the minimum value of the depth of the geothermal reservoir. Thus, the borehole should be cased to this depth.

GEOELECTRIC MODEL OF GEOTHERMAL RESERVOIR

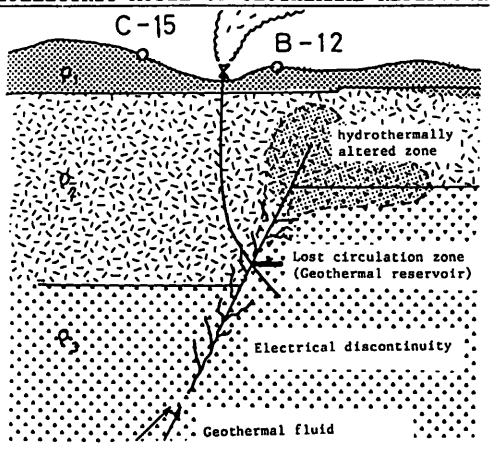

Fig. 7. Geoelectric model of the geothermal system.

From the preceding results, we may conclude that the geoelectric structure of the present geothermal reservoir system of Hatchobaru power plant could be explained by the model as shown in Fig. 7.

NUMERICAL MODELING

In order to test the applicability of one-dimensional inversion technique, the two-dimensional model study was made by the finite difference method. The apparent resistivity curves were calculated for a various model with two-dimensional resistivity changes such as a vertical fault, an inclined fault, a horizontal reservoir with the vertical fault, a vertical reservoir with the vertical fault, and so on.

At present, the model shown in Fig. 8 was considered to be an acceptable one because the simulated resistivity sounding curves are very similar in shape to those observed at stations B-12 and C-15.

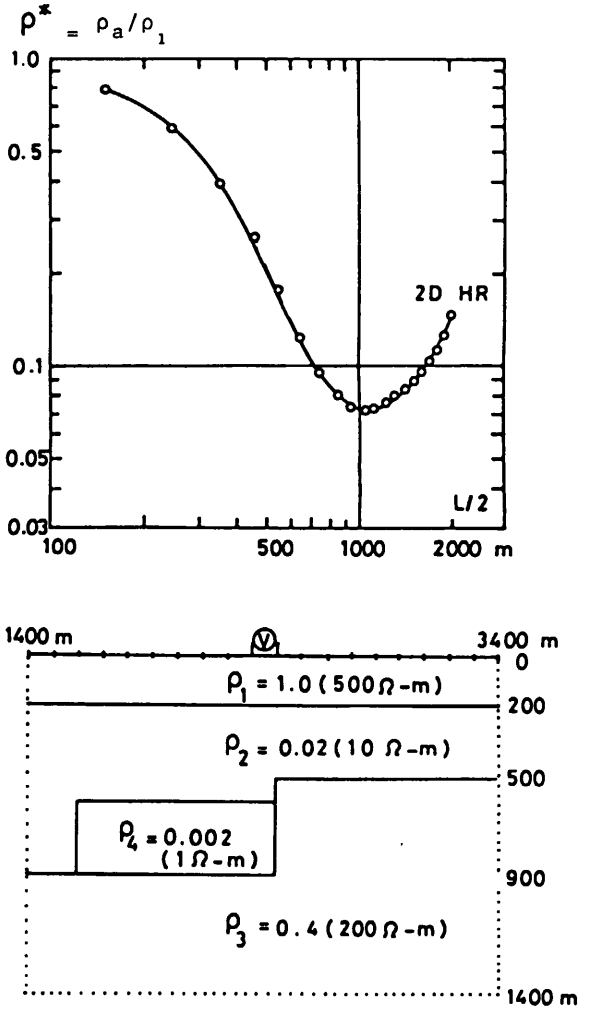

Fig. 8. Relative resistivity sounding curve for a two-dimensional model calculated by the finite difference method. Schlumberger sounding station is taken over the vertical fault.

INTERPRETATION OF VES CURVES OF LINE D

In this section we shall discuss the resistivity sounding data of line D in the southern part of Hatchobaru area. The area including the line D are expected to develop geothermal resources for the power plant, while at present there are no production wells within this area. From this reason, the resistivity sounding curves of line D were interpreted by the anisotropic and isotropic inversion methods. The results are expressed in a resistivity layer section as shown in Fig. 9.

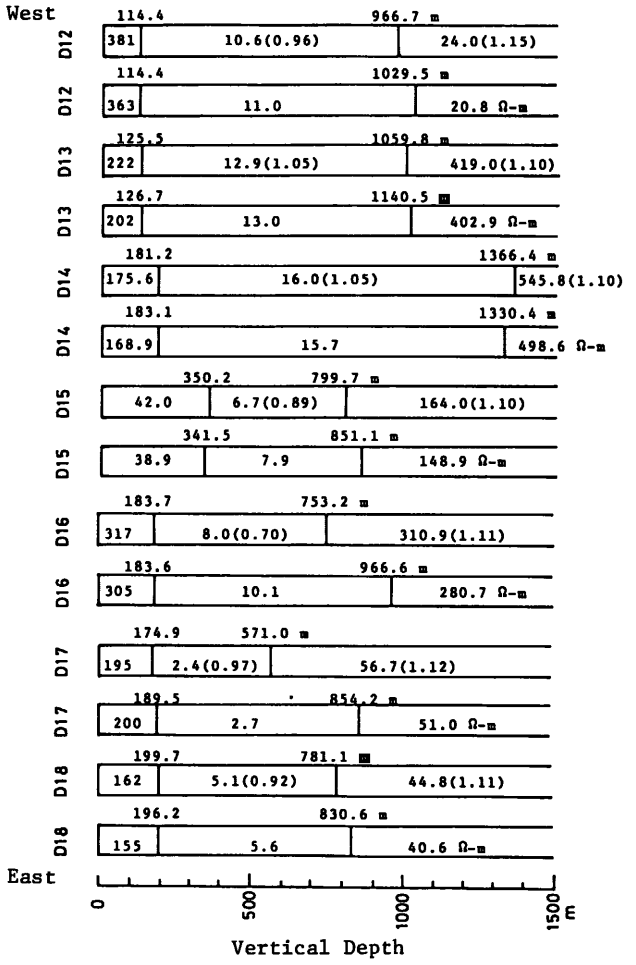

Fig. 9. Resistivity layer section of line D at Hatchobaru field.

The figure suggests that two promissing geothermal reservoirs which have a similar structure expressed by the geoelctric model of Fig. 7 exist in the regions of stations D16 - D17 and D17 - D18.

Judging from the ease to access of drilling operation, we came to conclude that the station D16 is the most promissing site for drilling in order to develop a further geothermal resources.

ANISOTROPIC COEFFICIENTS

In the actual field, from the definition of an anisotropic coeffcient by eq.(2), there is a possibility that α may be less than unity. This happens whenever the size and frequency of vertical cracks are sufficient to channel enough current vertically (Campbell, 1977).

From a geological viewpoint, a large difference of anisotropic coefficients from unity (isotropic case) suggests that the formation has zones of intense jointing and fracturing.

Fig. 10 shows the distribution of the anisotropic coefficients determined from the resistivity inversion. Generally, interpretation results of anisotropic resistivity inversion may be classified into the following four domain:

Domain	Anisotropic Coefficients	Cracks
I	$\alpha_\ell > 1$ and $\alpha_b > 1$	horizontal
II	$\alpha_\ell > 1$ and $0 < \alpha_b < 1$	mixed
III	$0 < \alpha_\ell < 1$ and $0 < \alpha_b < 1$	vertical
IV	$0 < \alpha_\ell < 1$ and $\alpha_b > 1$	mixed

According to this classification, it is found that all of VES curves obtained at Hatchobaru area show the presence of electrical anisotropy both in the low resistivity layer and electrical basement.

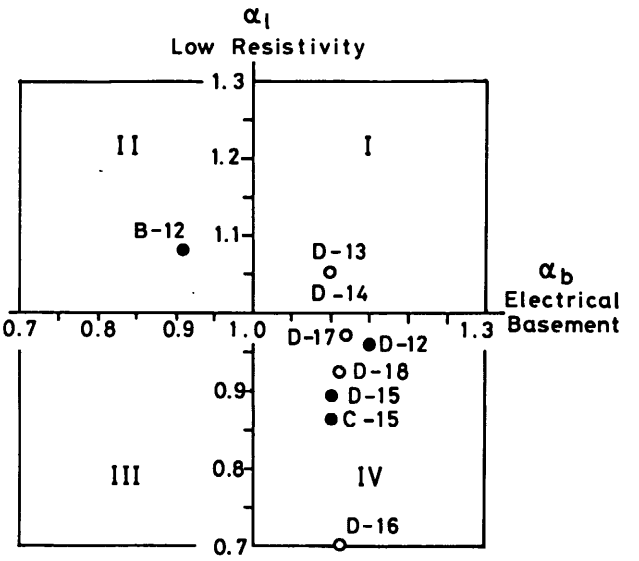

Fig. 10. Distribution of anisotropic coeffcients from the resistivity inversion. Solid circles were confirmed to be productive by the production or exploratory wells.

CONCLUSIONS

A new method of interpretation of VES curve was presented based on an anisotropic layered earth model. The method was applied to the VES data obtained in the vicinity of producing region and a virgin area, and the results of the former were compared with the drilling data of production wells in order to deduce a geoelectric model of the geothermal reservoir at Hatchobaru geothermal field.

It is relevant from this investigation that the present method provide more stable depth estimates to a geothermal reservoir and anisotropic coefficients.